

Topological constraints on magnetic field relaxation

Simon Candelaresi, & Axel Brandenburg

NORDITA, KTH Royal Institute of Technology and Stockholm University, Roslagstullsbacken
23, SE-10691 Stockholm, Sweden
and Department of Astronomy, AlbaNova University Center, Stockholm University, SE-10691
Stockholm, Sweden

Abstract.

Magnetic field relaxation is determined by both the field's geometry and its topology. For relaxation processes, however, it turns out that its topology is a much more stringent constraint. As quantifier for the topology we use magnetic helicity and test whether it is a stronger condition than the linking of field lines. Further, we search for evidence of other topological invariants, which give rise to further restrictions in the field's relaxation. We find that magnetic helicity is the sole determinant in most cases. Nevertheless, we see evidence for restrictions not captured through magnetic helicity.

Keywords. Magnetic field relaxation, magnetic helicity, field topology

1. Introduction

Geometry and topology of magnetic field lines fundamentally affect their dynamics (Woltjer 1958; Arnold 1974; Ruzmaikin *et al.* 1994; Taylor 1974; Del Sordo *et al.* 2010; Yeates *et al.* 2010, 2011). For instance, strongly tied field lines give rise to strong current sheets which then facilitate magnetic reconnection under which field lines brake and connect in a different way. Reconnection for its part, can give rise to ejections of plasma, which is of particular interest in the case of our Sun.

While the field's geometry has often been appreciated, its topology has received less attention. Loosely speaking, topology determines the field's linkage, while geometry its configuration in space. Any two field configurations which are topologically different cannot be transformed one into the other without breaking field lines, i.e. reconnection.

2. Magnetic helicity

Magnetic helicity density is the scalar product of the magnetic vector potential \mathbf{A} and the magnetic field \mathbf{B} , i.e.

$$h = \mathbf{A} \cdot \mathbf{B}. \quad (2.1)$$

Its integral over a closed or periodic system, the total magnetic helicity,

$$H = \int \mathbf{A} \cdot \mathbf{B} \, dV, \quad (2.2)$$

is a conserved quantity in ideal MHD and in the limit of vanishing magnetic resistivity (Woltjer 1958).

Topologically speaking, H is a quantifier for the mutual linkage of magnetic flux tubes and their internal twist (Moffatt 1969). Twisted and linked fields are severely restricted

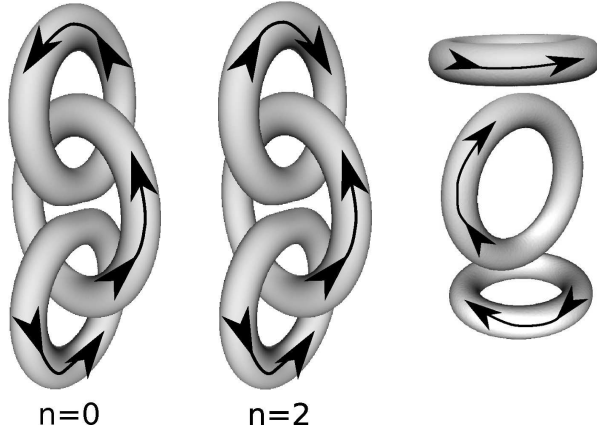


Figure 1. Iso surfaces of the magnetic energy for the initial magnetic field configurations. Arrows denote the direction of the field. The left configuration is non-helical, while the center one is helical. The right configuration was used as control run and is not helical.

in their dynamics, in particular their relaxation. Arnold (1974) first quantified this restriction in the realizability condition

$$E(k) = 2|H(k)|/k, \quad (2.3)$$

with the spectral magnetic energy $E(k)$, the spectral magnetic helicity $H(k)$, and the wave number k . It gives a lower bound for the magnetic energy in the presence of magnetic helicity. In its picturesque interpretation as linking of flux tubes it becomes clear why magnetic helicity imposes restrictions on the magnetic field decay given by equation (2.3). During relaxation, mutually linked field lines cannot freely evolve without magnetic reconnection. As long as reconnection is not aided by strong inflows of magnetic fields into the reconnection zone, it will not occur fast enough for any appreciable field change or energy loss. There exist, however, field topologies of linked magnetic field lines which are not helical and for which equation (2.3) has no effect.

In a first work we investigate whether the field's topology, as it is given by the linking and twisting of field lines, is the determining factor in relaxation, or whether the magnetic helicity content is the key quantity (Del Sordo *et al.* 2010). From the plethora of possible magnetic field configurations one of the simplest examples is chosen, which is a triple ring configuration of interlinked flux tubes (Fig. 1).

We solve the resistive MHD equations for a viscous, compressible and isothermal gas

$$\frac{\partial}{\partial t} \mathbf{A} = \mathbf{U} \times \mathbf{B} - \eta \mu_0 \mathbf{J}, \quad (2.4)$$

$$\frac{D}{Dt} \mathbf{U} = -c_s^2 \nabla \ln \rho + \frac{1}{\rho} \mathbf{J} \times \mathbf{B} + \mathbf{F}_{\text{visc}}, \quad (2.5)$$

$$\frac{D}{Dt} \ln \rho = -\nabla \cdot \mathbf{U}, \quad (2.6)$$

with the velocity \mathbf{U} , the molecular magnetic resistivity η , the susceptibility in vacuum μ_0 , the electric current density $\mathbf{J} = \nabla \times \mathbf{B}/\mu_0$, the isothermal speed of sound c_s , the density ρ and the advective time derivative $D/Dt = \partial/\partial t + \mathbf{U} \cdot \nabla$. Viscous effects are caught in $\mathbf{F}_{\text{visc}} = \rho^{-1} \nabla \cdot 2\nu \rho \mathbf{S}$, where ν is the kinematic viscosity, and \mathbf{S} is the traceless rate of strain tensor with components $S_{ij} = \frac{1}{2}(u_{i,j} + u_{j,i}) - \frac{1}{3}\delta_{ij} \nabla \cdot \mathbf{U}$. Commas denote

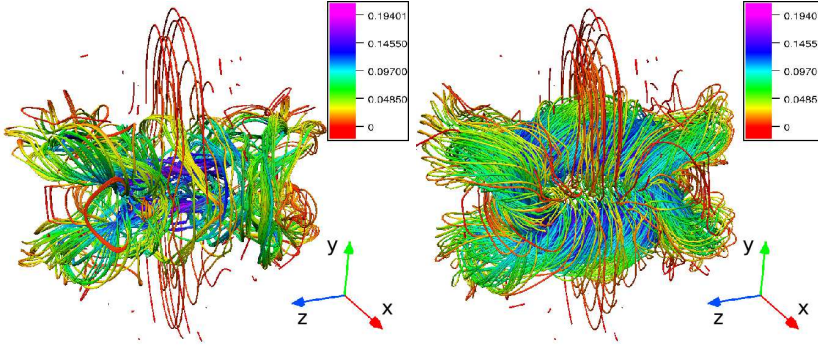


Figure 2. Magnetic field lines for the two interlocked triple ring configurations after 4 Alfvénic times of resistive decay. The non-helical initial configuration (left panel) loses its shape quicker than the helical configuration (right panel).

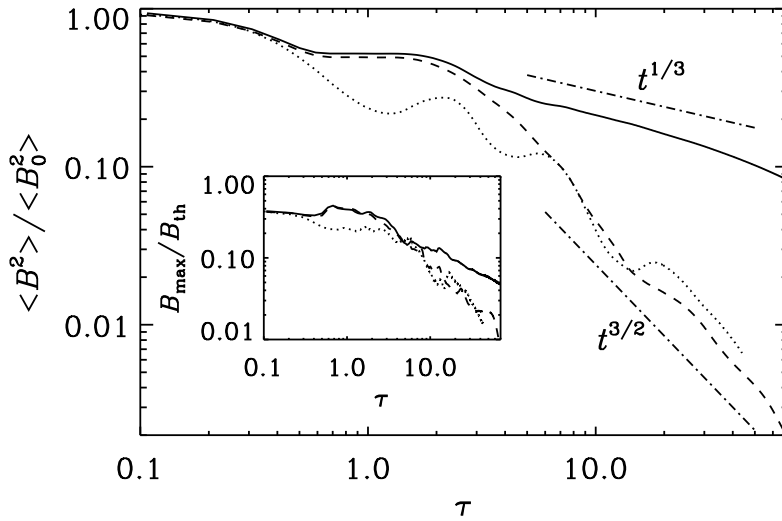


Figure 3. Normalized magnetic energy evolution for the helical linked rings (solid line), non-helical linked rings (dashed line) and unlinked rings (dotted line).

partial derivatives. Initial magnetic fields represent either of the three configurations in Fig. 1, while the initial velocity vanishes in the whole domain and the initial density is unity. Boundary conditions are chosen as periodic in order to conserve magnetic helicity.

From the time evolution of the magnetic field lines it becomes clear that linking alone cannot hinder the fast decay of the magnetic energy (Fig. 2, left panel). In the presence of magnetic helicity, however, the decay is slowed down considerably (Fig. 2, right panel). Our control setup with non-interlinked flux tubes shows an energy decay characteristics which is very close to the interlinked non-helical field (Fig. 3). The helical configuration, on the other hand, shows a much slower decay rate. From this we conclude that magnetic helicity, rather than linking of flux tubes, determines the field's dynamics.

In the same fashion we test the importance of the field's linkage and knottedness for non-helical configurations with other highly non-trivial topologies. Initial fields are the IUCAA knot (Fig. 4, left panel), which, in the Alexander-Briggs notation, is the 8₁18 knot, and the Borromean rings (Fig. 4, right panel), after the emblem of the north Italian

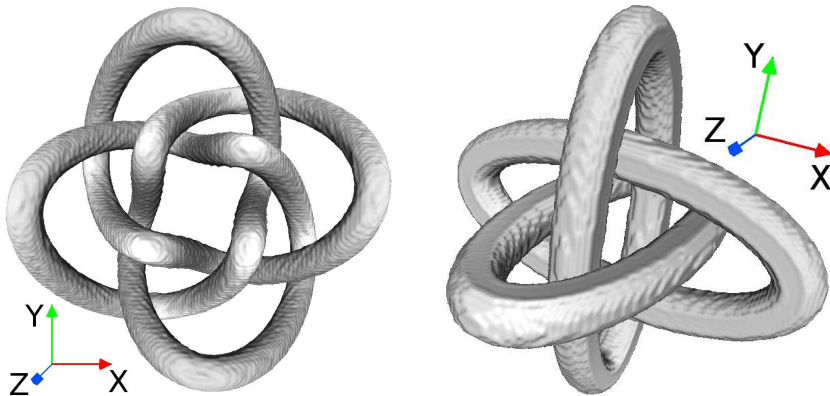


Figure 4. Iso surfaces of the initial magnetic energy for the IUCAA knot (left panel) and the Borromean rings (right panel).

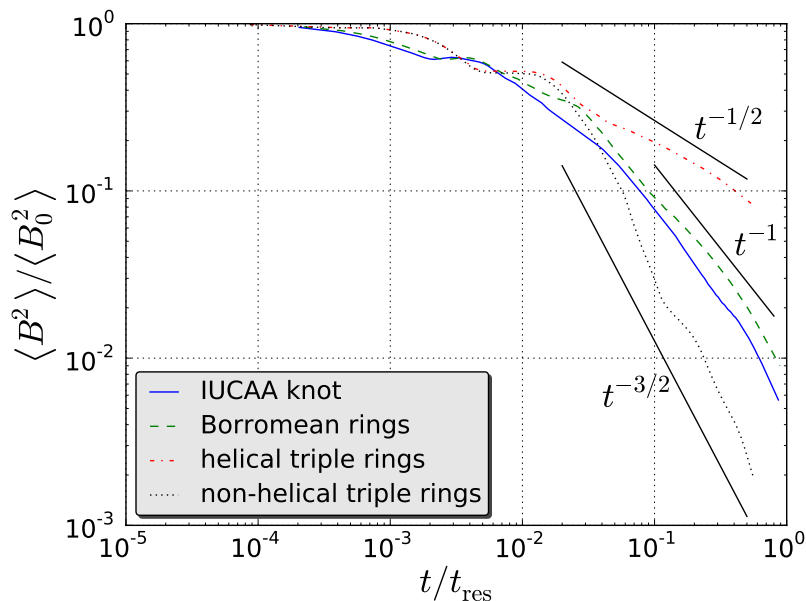


Figure 5. Comparison of the magnetic energy evolution for different initial field configurations.

aristocratic house of Borromeo. We compare the magnetic energy evolution with the triple ring configurations and find that both, the IUCAA knot and the Borromean rings, show an intermittent power law in the energy decay (Fig. 5). This allows for speculations about higher order topological invariants, which are non-zero for those field configurations and impose additional restrictions on the field's dynamics; see e.g. Ruzmaikin *et al.* (1994).

3. Beyond magnetic helicity

There exists an infinite number of topological invariants for three-dimensional vector fields. Applications on MHD have been, nevertheless, very limited and successful in only a few attempts. Two invariants of third and fourth order in \mathbf{B} are finite for the Borromean

rings (Ruzmaikin *et al.* 1994). Their definition is, nevertheless, limited to distinct flux tubes which do not overlap. In resistive MHD magnetic field diffuses and an initially confined field will occupy the whole space.

One way around this hitch is by using the fixed point index (see e.g. Frankel (2004); Yeates *et al.* (2010)), which in turn, is only applicable to fields with a preferential direction, like in toroidal fields, or a field with a positive z -component. In the latter case one can define a mapping between the bottom and top boundaries by tracing the field lines, resulting in the field line mapping,

$$\mathbb{R}^2 \rightarrow \mathbb{R}^2, \quad (3.1)$$

$$(x, y) \rightarrow \mathbf{F}(x, y), \quad (3.2)$$

with the initial point (x, y) at $z = 0$. Note that $\mathbf{F}(x, y)$ is bijective.

Fixed points are those points for which $\mathbf{F}(x, y) = (x, y)$. There can be infinitely or finitely many, with at least one fixed point. Considering the fixed point's neighborhood in the xy plane we can determine its sign. Depending if $\mathbf{F}^x(x, y) > x$ and $\mathbf{F}^y(x, y) > y$, a color is assigned; for $\mathbf{F}^x(x, y) < x$ and $\mathbf{F}^y(x, y) > y$ a different color is assigned, likewise for the other cases. The sequence of these colors around the fixed point determines its sign t_i , where $t_i \in \{-1, 1\}$. Summing over all fixed points yields the fixed point index (Brown 1971; Frankel 2004)

$$T = \sum_i t_i, \quad (3.3)$$

which is a conserved quantity in ideal MHD (Brown 1971).

Simulations using the fixed point index as constraining quantity were performed by Yeates *et al.* (2010, 2011), where they observed a constraint relaxation of magnetic fields. Their equilibrium state turned out to be of higher energy than that proposed by Taylor (1974).

4. Conclusions

From resistive MHD simulations of relaxing interlinked magnetic fields it becomes apparent that magnetic helicity, rather than actual linkage, determines the field's relaxation properties. The decaying IUCAA knot and Borromean rings show some intermittent decline speed for the magnetic energy. This suggests that there might be higher order topological invariants, which impose restrictions on the field's dynamics. An example of such invariants is the fixed point index, which is conserved in ideal MHD and is shown to impose further restrictions on relaxation.

References

- Arnold, V. I. 1974, *Sel. Math. Sov.*, 5, 327
 Brown, R. F. 1971, *The Lefschetz Fixed Point Theorem* London: Scott Foresman
 Del Sordo, F., Candelaresi, S. & Brandenburg, A. 2010, *Phys. Rev. E*, 81, 036401
 Frankel, T. 2004, *The Geometry of Physics* Cambridge: Univ. Press
 Moffatt, H. K. 1969, *J. Fluid Mech.*, 35, 117
 Ruzmaikin, A. & Akhmetiev, P. 1994, *Phys. Plasmas*, 1, 331
 Taylor, J. B. 1974, *PRL*, 33, 1139
 Woltjer, L. 1958, *PNAS*, 44, 833
 Yeates, A. R., Hornig, G. & Wilmot-Smith, A. L. 2010, *PRL*, 105, 085002
 Yeates, A. R. & Hornig, G. 2011, *JPA*, 44, 265501